

## A Theoretical Analysis of the Operation of Ionization Chambers and Pulse Amplifiers

E. A. JOHNSON AND A. G. JOHNSON, *Department of Terrestrial Magnetism, Carnegie Institution of Washington*

(Received April 28, 1936)

The noise level of a system composed of an ionization chamber and a linear amplifier is calculated as a function of the input circuit parameters and the characteristics of the amplifier. The frequency spectrum of a pulse caused when an ionizing particle passes through the ionization chamber is also calculated as a function of the circuit parameters and the collection time. From this analysis the shape of the output pulse is calculated as a function of the frequency

characteristic of the amplifier. It is concluded that the cut-off frequencies of the amplifier for optimum pulse shape and amplitude depend upon the collection time. The signal to noise ratio is calculated for the case of optimum pulse shape. By proper choice of tubes it is shown that it should be possible to count 100 ion pairs and that for a 1-cm deep chamber and fast protons the signal to noise ratio should be 38 : 1.

**M**OST of the information available concerning the design of ionization chambers and their associated circuit and pulse amplifier have been of a strictly empirical nature. It is the purpose of this analysis to indicate more definitely the important factors which limit the sensitivity of this type of detector in the investigation of the products of nuclear disintegrations. The problem is essentially one of determining the effect of circuit parameters and the characteristics of the amplifier used upon the signal to noise ratio.

In the design of an amplifier for the measurement of voltages whose amplitude is of the same order of magnitude as the noise of the first tube and its associated input circuit, the ratio of signal voltage to noise voltage depends upon their relative frequency spectrum and the transfer characteristics of the amplifier. In order to design an amplifier for the measurement of pulses from an ionization chamber, therefore, it is necessary to determine the frequency spectrum of a pulse, and the frequency spectrum of the noise from the input circuit and first tube. Before considering the limitations imposed in practice by tube characteristics, these two frequency spectra will be determined.

There are three principal sources of noise<sup>1</sup> from a circuit of the type shown in Fig. 1 which is the equivalent circuit of an ionization chamber and the first stage of the amplifier. The noise is due to thermal noise from the resistance, shot noise from the grid current in the resistance-capacity network, and the zero noise of the tube. In Fig. 1,  $C$  is the combined

capacity of the ionization chamber, tube, and wiring, and  $R$  is the resistance in the grid circuit due to the internal dynamic grid resistance and any external grid resistance.

In the analysis that follows an ideal amplifier is assumed which has constant gain between the frequencies  $f_1$  and  $f_2$  and zero gain outside of this band, and no phase distortion in the band. Such an amplifier is difficult to obtain in practice, but the conclusions reached will be only slightly affected by the approximation.

### CALCULATION OF NOISE LEVEL

The thermal noise from the input circuit due to thermal agitation of charge in the resistance is given by

$$\overline{E_r}^2 = 4kTR \int_{f_1}^{f_2} df / (1 + 4\pi^2 R^2 C^2 f^2), \quad (1)$$

where  $K$  is Boltzmann's constant,  $T$  is the absolute temperature. By integrating

$$E_r^2 = (4kT/2\pi C) \tan^{-1} [2\pi RC(f_2 - f_1) / (1 + 4\pi^2 R^2 C^2 f_2 f_1)]. \quad (2)$$

The shot noise in the input circuit due to statistical fluctuations in the grid current  $I_g$  of the first tube is given by

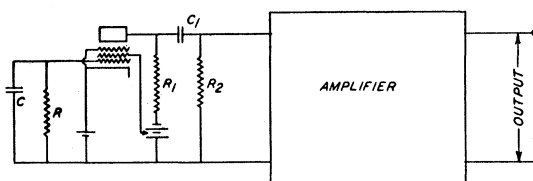


FIG. 1. Input stage of pulse amplifier.

<sup>1</sup> G. L. Pearson, *Physics* 5, 233 (1934).

$$\overline{E_s^2} = 2eI_g R^2 \int_{f_1}^{f_2} df / (1 + 4\pi^2 R^2 C^2 f^2), \quad (3)$$

$$E_s^2 = (2eI_g R / 2\pi C) \tan^{-1} [2\pi RC(f_2 - f_1) / (1 + 4\pi^2 R^2 C^2 f_1^2)], \quad (4)$$

where  $e$  is the electronic charge and  $I_g = |I_+| + |I_-|$  where  $|I_+|$  and  $|I_-|$  are the absolute magnitude of positive and negative components of grid current. From (2) and (4) we obtain the relation for  $T = 300^\circ\text{K}$ ,

$$\overline{E_s^2} = (19.4I_g R) \overline{E_r^2}. \quad (5)$$

The third source of noise is due to the zero noise level in the tube itself and is given by:

$$\overline{E_t^2} = 4kT \int_{f_1}^{f_2} R_t df \quad (6)$$

$$= 4kTR_t(f_2 - f_1), \quad (7)$$

where  $R_t$  is the resistance which, if placed in the input of the first tube, would give the same reading in the output meter of the amplifier if there were no noise from the tube itself. The total mean square voltage is then given by

$$\begin{aligned} \overline{E_n^2} &= \overline{E_s^2} + \overline{E_r^2} + \overline{E_t^2}, \\ E_n^2 &= 4kT \left\{ (1/2\pi C) \tan^{-1} \right. \\ &\quad \left. [2\pi RC(f_2 - f_1) / (1 + 4\pi^2 R^2 C^2 f_1^2)] \right. \\ &\quad \left. \times [1 + 19.4I_g R] + R_t(f_2 - f_1) \right\}. \quad (8) \end{aligned}$$

The case of interest to us is when  $2\pi f_2 RC > 2\pi f_1 RC \gg 1$  and for this condition Eq. (8) reduces to

$$\begin{aligned} \overline{E_n^2} &= 4kT(f_2 - f_1) \\ &\quad \times [R_t + (1 + 19.4I_g R) / RC^2 4\pi^2 f_1 f_2]. \quad (9) \end{aligned}$$

If we plot  $\overline{E_n^2}$  vs.  $R$  from Eq. (8) we obtain a curve of the type shown in Fig. 2 where the circuit constants assumed are:  $f_1 = 500$  c.p.s.,  $f_2 = 5000$  c.p.s.,  $C = 10^{-11}$  farad,  $I_g = 10^{-10}$  ampere and  $R_t = 20,000$  ohms.

We see that when  $R$  is very small the zero noise from the tube itself predominates and determines the noise level. As  $R$  is increased the thermal noise increases and is the determining factor and would increase indefinitely except for

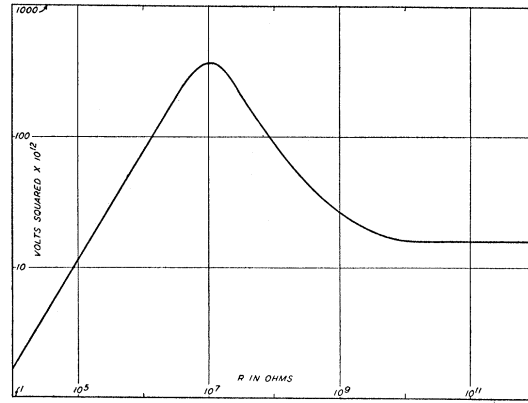


FIG. 2. Input noise as a function of input resistance.

the shunting effect of the capacity  $C$ . Because of the shunting effect of  $C$  which becomes more effective as  $R\omega C$  is large compared to unity, the thermal noise decreases and the total noise would again be reduced to the noise level of the tube alone were it not for the fact that the shot noise due to the grid current becomes of importance. The shot noise decreases with an increase in  $R$  to an asymptotic value and the minimum noise is given by

$$\overline{E_n^2} = 4kT(f_2 - f_1) [R_t + 19.4I_g / 4\pi^2 C^2 f_1 f_2] \quad (10)$$

and is determined only by the zero noise of the tube, by its grid current and by the parameters  $C$ ,  $f_1$ , and  $f_2$  and does not depend upon  $R$  if  $R$  is sufficiently large.

From (10) we conclude that the noise level is made a minimum by choosing a tube with as low values of grid current and of zero noise as possible and making  $R$  as large as possible. The parameters  $f_1$ ,  $f_2$ , and  $C$  also determine the noise level but we shall see that they are fixed by the requirements of pulse definition.

#### FOURIER ANALYSIS OF PULSE

The voltage on the grid of the first tube due to the discharge of the ionization chamber is given by<sup>2</sup>

$$\begin{aligned} E_g &= 0, & -\infty < t < 0, \\ E_g &= (Rq/\lambda)(1 - e^{-t/RC}), & 0 < t < \lambda, \\ E_g &= (Rq/\lambda)(1 - e^{-\lambda/RC})e^{-(t-\lambda)/RC}, & \lambda < t < +\infty, \end{aligned} \quad (11)$$

<sup>2</sup>G. Ortner and G. Stetter, Zeits. f. Physik 54, 449 (1929).

where  $q$  is the charge collected on the plate of the ionization chamber connected to the first stage of the amplifier, due to the passage of a single ionizing particle through the chamber, and  $\lambda$  is the time required to sweep the ions to the plate.

$E_g(t)$  is continuous and the integral  $\int_{-\infty}^{+\infty} E_g(t) dt$  is absolutely integrable. Thus the conditions for a Fourier integral are satisfied. The spectrum of (11) is then given by

$$G(\omega) = (1/(2\pi)^{\frac{1}{2}})(Rq/\lambda) \left[ \int_0^\lambda \epsilon^{-i\omega t} dt - \int_0^\lambda \epsilon^{-(1/RC+i\omega)t} dt + \epsilon^{\lambda/RC} \int_\lambda^\infty \epsilon^{-(1/RC+i\omega)t} dt - \int_\lambda^\infty \epsilon^{-(1/RC+i\omega)t} dt \right] \quad (12)$$

Integrating and substituting the limits we have

$$G(\omega) = A(1 - \cos \omega\lambda + j \sin \omega\lambda) / j\omega(1 + j\omega RC) = A(1 - \epsilon^{-i\omega\lambda}) / j\omega(1 + j\omega RC), \quad (13)$$

where  $A = Rq/(2\pi)^{\frac{1}{2}}\lambda$ .

We note that the frequency spectrum is of the oscillating type with an envelope that approaches  $Rq/(2\pi)^{\frac{1}{2}}$  asymptotically at the origin. The average energy per cycle consequently falls off at the higher frequencies and it should be noted that there is no maximum in the frequency spectrum corresponding to a frequency  $1/4\lambda$  as is commonly supposed. The effect of varying  $\lambda$  is merely to change the number of oscillations inside of the envelope of the energy spectrum within a given frequency range. The effect of changing  $RC$  is to shift the envelope to higher or lower frequencies as  $RC$  is decreased or increased.

The best means of evaluating the effect of the circuit parameters is to determine the time response in the output of the amplifier. The time response in the output of the amplifier referred to the input, i.e., divided by the gain of the amplifier, is given by

$$E(t) = A \int_{\omega_1}^{\omega_2} (1 - \epsilon^{-i\omega\lambda}) \epsilon^{i\omega t} d\omega / j\omega(1 + j\omega RC). \quad (14)$$

It can easily be shown that the value of  $E(t)$  will be a maximum when  $\omega_2 RC > \omega_1 RC \gg 1$  and (14) becomes

$$E(t) = A(t - \lambda) / RC \int_{y_1}^{y_2} \epsilon^{iy} dy / y^2 - At / RC \int_{x_1}^{x_2} \epsilon^{ix} dx / x^2, \quad (15)$$

where  $x = \omega t$  and  $y = \omega(t - \lambda)$ . By integrating and substituting the limits,

$$E(t) = \{A(t - \lambda) / RC\} \{[\cos \omega_1(t - \lambda)] / \omega_1(t - \lambda) - [\cos \omega_2(t - \lambda)] / \omega_2(t - \lambda) + Si\omega_1(t - \lambda) - Si\omega_2(t - \lambda)\} - \{At / RC\} \{[\cos \omega_1 t] / \omega_1 t - [\cos \omega_2 t] / \omega_2 t + Si\omega_1 t - Si\omega_2 t\} + \{jA(t - \lambda) / RC\} \{[\sin \omega_1(t - \lambda)] / \omega_1(t - \lambda) - [\sin \omega_2(t - \lambda)] / \omega_2(t - \lambda) - Ci\omega_1(t - \lambda) + Ci\omega_2(t - \lambda)\} - \{jAt / RC\} \{[\sin \omega_1 t] / \omega_1 t - [\sin \omega_2 t] / \omega_2 t - Ci\omega_1 t + Ci\omega_2 t\}. \quad (16)$$

In any practical case the amplitude of the complex part is small and can be neglected, and (16) can be written:

$$E(t) = [q/C\lambda(2\pi)^{\frac{1}{2}}][t(X - Y) + \lambda Y] = [q/C(2\pi)^{\frac{1}{2}}]E(\lambda, t), \quad (17)$$

where

$$E(\lambda, t) = [t(X - Y) + \lambda Y] / \lambda, \quad X = X_1 - X_2, \\ X_n = [\cos \omega_n t] / \omega_n t + Si\omega_n t, \quad Y = Y_1 - Y_2, \\ Y_n = [\cos \omega_n(t - \lambda)] / \omega_n(t - \lambda) + Si\omega_n(t - \lambda).$$

Then the ratio of signal to the root-mean-square value of noise is given by

$$E(t) / E_n = qE(\lambda, t) 3.14 \times 10^9 / ((f_2 - f_1) \times [R_t C^2 + (1 + 19.4 I_g R) / 4\pi^2 R f_1 f_2])^{\frac{1}{2}}. \quad (18)$$

One of the additional requirements in counting pulses is that the amplitude of all except the first pulse in the train of output pulses due to the causal input pulse be small. This requirement is a fundamental one, since otherwise a single pulse

\* The best tables of this function are found in Vol. I of the *Mathematical Tables* published by the British Association for the Advancement of Science.

might be counted more than once in the output, and the sharpness of the first output pulse is a deciding factor in the resolution of the counting system.

From a consideration of (18) we can now determine the relative noise level when all of the parameters are given. Before discussing this equation it is necessary to consider the function  $E(\lambda, t)$ .

$E(\lambda, t)$  depends only upon  $f_1, f_2, \lambda,$  and  $t$ .

In order to determine its dependence upon these quantities  $E(\lambda, t)$  has been plotted for a large number of different combinations of the parameters. A typical family of curves of  $E(\lambda, t)$  is shown in Fig. 3 for various values of  $f_2$  with  $f_1=240$  c.p.s. and  $\lambda=2 \times 10^{-4}$  second. It is to be noted that only the first pulse is essentially affected by the upper band limit, the secondary and negative pulses are primarily determined by the lower band limit. This does not hold exactly

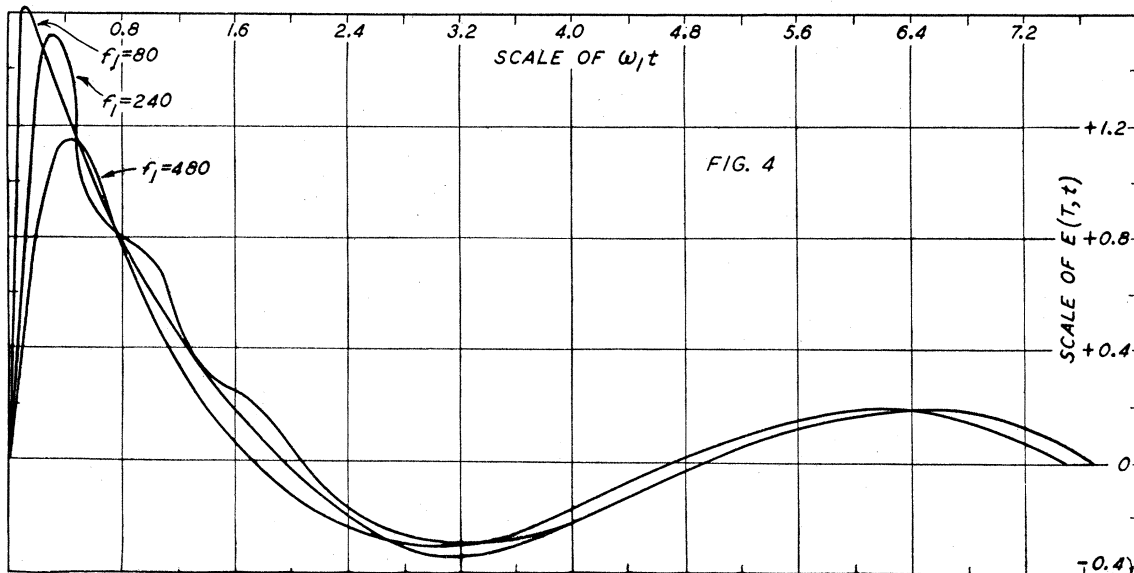
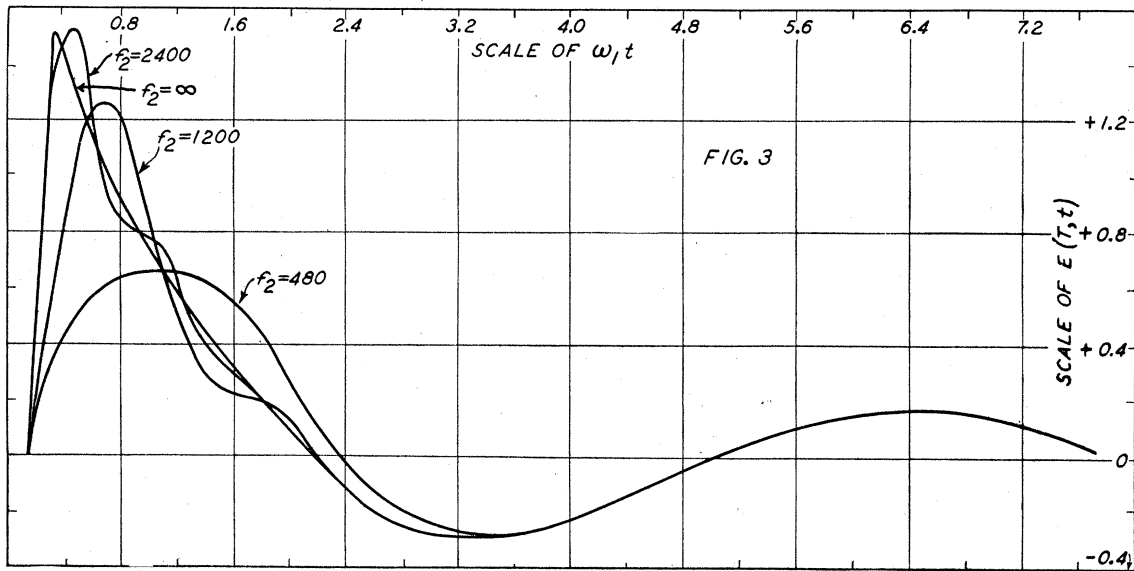


FIG. 3. Pulse shape as a function of upper cut-off ( $T=2 \times 10^{-4}$ ;  $f_1=240$  c.p.s.).  
 FIG. 4. Pulse shape as a function of lower cut-off ( $T=2 \times 10^{-4}$ ;  $f_2=2400$  c.p.s.).

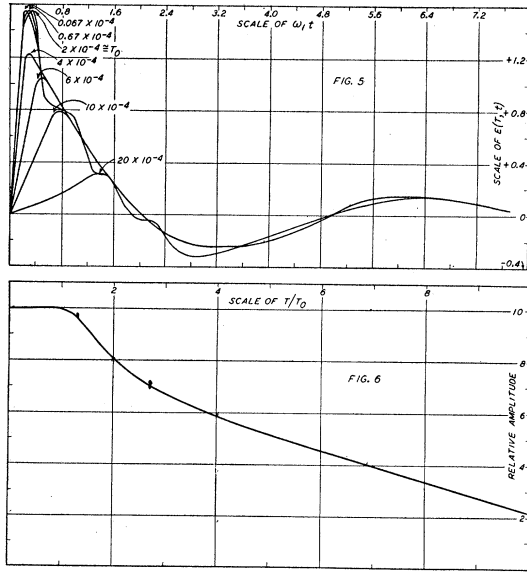


FIG. 5. Pulse shape as a function of collection time ( $f_1=240$  c.p.s.;  $f_2=2400$  c.p.s.).

FIG. 6. Pulse amplitude as a function of collection time ( $f_2=10f_1$ ;  $T_0=2/f_2$ ).

when  $f_2$  is very near to  $f_1$  but does for the cases in which we are interested, since from Fig. 3 it is evident that  $f_2$  must be large compared to  $f_1$ . However, it is seen that no appreciable change occurs if  $f_2$  is increased beyond 2400 c.p.s. in this particular case. Similar families of curves are obtained for different values of  $f_1$  and  $\lambda$  and in each case the critical value of  $f_2$  occurs at  $f_2=1/2\lambda$ .

Fig. 4 shows a similar family of curves of  $E(\lambda, t)$  vs.  $t$  for various values of  $f_1$  and with  $f_2=2400$  c.p.s. and  $\lambda=2 \times 10^{-4}$  second. From these curves and similar families we conclude that the optimum value of  $f_1$  is obtained when  $f_1$  equals  $1/20\lambda$ .

The optimum pulse shape is thus seen to be obtained when  $f_2$  equals  $10f_1$  and  $f_2=1/2\lambda$ . Fig. 5 is a plot of  $E(\lambda, t)$  vs.  $t$  for various values of  $\lambda$  and with  $f_1=240$  c.p.s. and  $f_2=2400$  c.p.s., and shows the effect of variation of collection time for a fixed band width. The same data are plotted in a different way in Fig. 6 in which the maximum amplitude of  $E(\lambda, t)$  is plotted against  $\lambda/\lambda_0$  where  $\lambda_0=1/2f_2$ . This curve is perfectly general and it is seen that no further change in pulse amplitude occurs if  $\lambda$  is less than the critical collection time  $\lambda_0$ . From this discussion we see that if the longest collection time of the ionization chamber

is known the characteristics of the amplifier are determined.

In any practical case the collection time  $\lambda$  is determined by the geometry and the gas of the ionization chamber as well as the collection voltage. It should be noted that the curve of Fig. 6 provides a means of determining the collection time of a chamber, for since  $\lambda$  can be varied by varying the collection voltage across the chamber, the voltage at which the critical collection time is obtained can be determined, and the collection time at any other voltage found from the curve.

If we assume the amplifier  $f_2=10f_1$  and  $f_2=1/2\lambda$  and write for  $E(\lambda, t)$  its maximum value we obtain as a measure of the signal to noise ratio

$$E_m(t)/E_n = q7.3 \times 10^9 (\lambda / [R_t C^2 + \lambda^2] \times (1 + 19.4 I_g R) / 0.99 R)^{1/2} \quad (19)$$

If we differentiate (19) with respect to  $\lambda$  and set equal to zero in order to find the optimum value of  $\lambda$  for a given set of tube and circuit parameters, we find that (19) is a maximum when  $\lambda$  has the value:

$$\lambda = C(0.99 R_t R / (1 + 19.4 I_g R))^{1/2} \quad (20)$$

The maximum signal-to-noise ratio is then given by

$$[E_m(t)/E_n]_{\max} = N11.3 \times 10^{-10} \times (R/R_t C^2 (1 + 19.4 I_g R))^{1/2}, \quad (21)$$

where  $N$  is the equivalent number of singly charged ion pairs collected by the chamber. If we regard  $R_t$  and  $I_g$  as parameters fixed by the tube from (21) the signal-to-noise ratio is made a maximum when  $C$  is a minimum and  $R$  is large. If the tube is operated with a floating grid the factor  $(R/R_t C^2 (1 + 19.4 I_g R))^{1/2}$  is a measure of the merit of the tube. In this particular case  $R$  is the dynamic grid resistance at the floating potential, and  $C$  is the sum of the ionization chamber capacity and the dynamic input capacity of the tube, and is given nearly enough by

$$C = C_i + C_{gj} + (1 + \mu_e) C_{gp} + C_s \quad (22)$$

where:

$C_i$  = ionization chamber capacity,  
 $C_{gf}$  = grid-to-filament capacity,  
 $C_{gp}$  = grid-to-plate capacity,  
 $C_s$  = stray capacity to ground,  
 $\mu_e$  = effective voltage amplification of first stage.

In triodes  $R_t$  may be as low as 4000 ohms<sup>1</sup> while in pentodes the best values of  $R_t$  usually fall between 10,000 to 20,000 ohms.<sup>1, 3</sup> However, in triodes the value of  $(1 + \mu_e)C_{gp}$  is usually prohibitively large so that pentodes are to be preferred in spite of their higher values of  $R_t$ .

For example, if we assume an ionization chamber plus stray capacity of 5 mmf, the relative merit of the RCA 238; the WE 259-B and WE 262-A has been calculated from published data and is given in Table I.

The 238 and 259-B are pentodes and the 262-A is a triode. There are a large number of other types of tubes, both pentodes and triodes with factors of merit in the same range of values; and the pentodes in general have the higher values.

Since the collection time  $\lambda$  determines the amplifier which in turn determines the resolution, for fast counting rates it may be desirable to operate at a different value of  $\lambda$  than the one that gives the best noise level. For this case from (19) we see that the best ratio of signal to noise is still obtained when  $R_t$  and  $C$  are a minimum and  $R$  is large. When counting fast protons it may not be necessary to keep the secondary extremely low compared to the first pulse, and in that case the signal to noise may be improved slightly by the use of a narrower band width.

By a careful choice of tubes it may be expected that the factor of merit of the input tube may be increased beyond the values given in Table I. If the circuit of Fig. 1 is used and a tube with the constants  $R_t = 10,000$  ohms,  $C = 10^{-11}$  farad,  $I_g = 10^{-13}$  ampere, and an input resistance of  $10^{12}$  ohms is used, the factor of merit will be

TABLE I. *Relative merit of several input tubes for pulse amplifiers.*

| TUBE     | $R_t$ | $C$<br>$\times 10^{12}$ | $R$<br>$\times 10^{-10}$ | $I_g$<br>$\times 10^{11}$ | $(R/R_t C^2 (1 + 19.4 I_g R))^{\frac{1}{2}}$<br>$\times 10^{-6}$ |
|----------|-------|-------------------------|--------------------------|---------------------------|--|
| RCA 238  | 14000 | 14                      | 5                        | 0.2                       | 8.9  |
| WE 259-B | 19800 | 11                      | 1.2                      | 0.8                       | 6.5  |
| WE 262-A | 7700  | 28                      | 0.8                      | 1.8                       | 4.3  |

<sup>3</sup> E. A. Johnson and C. Neitzert, Rev. Sci. Inst. 5, 196 (1934).

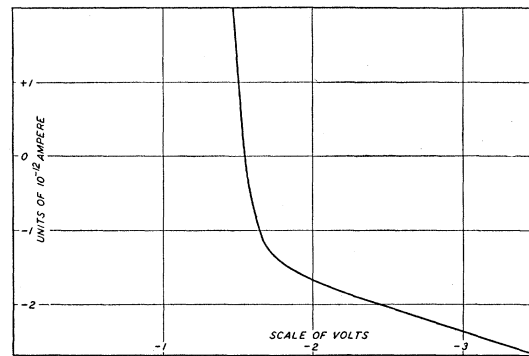


FIG. 7. Grid voltage vs. grid current curve of RCA type 38 tube.

$24 \times 10^6$ . From Eq. (21) if we assume that pulses whose amplitude is twice the mean noise level can just be detected, the minimum number of ion pairs that can be counted will be approximately 100. If we assume that fast protons produce 2000 ion pairs per centimeter of path, the signal-to-noise ratio for a one-cm deep ionization chamber will be 38 : 1 from Eq. (21) for fast protons and will be higher for slow protons and alpha-particles.

The circuit proposed in Fig. 1 has several advantages. If we consider the curve of  $E_g$  vs.  $I_g$  of the 238, from Fig. 7 we see that by operating at the point  $E_g = -2$  volts instead of at the floating potential the grid current is reduced to about half, since the electronic component is reduced to practically zero. The resistance of the circuit is practically the external resistance at  $E_g = -2$  volts since the dynamic resistance is very large. The noise level can consequently be improved slightly by the use of this circuit. It has one further advantage as is shown by the following analysis.

If  $RC$  is large and the number of impulses large, the grid will assume a voltage different from the voltage with no signal impressed. We assume first that the resistance in the grid circuit remains constant. It must be pointed out that this may be far from the actual circumstance, and may seriously affect the operating conditions.

We assume that each pulse decays as

$$E\epsilon^{-t/RC} \quad \text{where} \quad E = Rq(1 - \epsilon^{-\lambda/RC})\epsilon^{\lambda/RC}/\lambda. \quad (23)$$

If the pulses occur at an average interval of  $1/n$ ,

then the voltage of the grid at any time  $t$  will be

$$V = E[\epsilon^{-t/RC} + \epsilon^{-(t-1/n)/RC} + \epsilon^{-(t-2/n)/RC} + \dots].$$

Assuming a large number of pulses, the grid will be driven to a voltage:  $V = E/(\epsilon^{1/nRC} - 1) = nRCE$  since  $nRC$  will usually be large compared to unity.

$V$  may be of the order of 0.1 volt if the counting rate is high, when counting alpha-particles. With a floating grid, if we consider the curve of  $E_g$  vs.  $I_g$  of Fig. 7 it is seen that if the sense of  $V$  is such as to make the grid more negative  $I_g$  is decreased and  $R_g$  is increased. This results in an increase in  $V$  which carries the operating point still further negative, and the process continues until the grid voltage is driven so far negative that the tube becomes inoperative. For this reason the ionization chamber collection voltage is applied so that  $V$  drives the grid positive. However, this increases  $I_g$  and decreases  $R_g$  and the grid voltage is established at a new equilibrium at a more positive voltage, with  $I_g$  greater and  $R_g$  less than with no signal impressed.

Both of these factors result in a decrease in the signal to noise ratio which may be quite appreciable.

The circuit of Fig. 1 can be used to prevent this condition either by manually correcting for the change in grid bias at high counting rates, or by automatically biasing the grid.

In conclusion it should again be pointed out that this analysis holds only when an amplifier which has no phase distortion is used. If unequal phase changes occur between the frequency components during amplification, they will not add in the output to give a maximum signal, but interference will take place which will result in a decreased signal. It is therefore essential that the overall characteristic of the amplifier shall contain no phase distortion.

The authors are indebted to Dr. John A. Fleming, the Director of the Department of Terrestrial Magnetism, for the opportunity to carry on this investigation, and to Dr. L. C. Van Atta and Dr. L. R. Hafstad for criticism of the manuscript.

## Magnetization of Nickel Under Compressive Stresses and the Production of Magnetic Discontinuities

C. W. HEAPS, *Rice Institute*

(Received May 26, 1936)

When nickel is compressed its hysteresis loop approaches a rectangular shape. Several curves for stresses increasing up to the elastic limit have been obtained. At the maximum stress the steep part of the loop is still not vertical and the Barkhausen effect is not appreciably changed by the pressure. Much smaller stresses in an elastically bent wire produce large magnetic discontinuities, hence the existence of contiguous compressed and stretched regions appears to be necessary for the production of the large discontinuities.

WHEN a straight piece of nickel wire is bent into the arc of a circle large discontinuities of magnetization are found to appear in its hysteresis loop.<sup>1</sup> It has been supposed that a discontinuity of this kind is caused by the sudden and complete reversal of the saturated magnetization of the compressed region of the wire. The compressed nickel is believed<sup>2</sup> to have an approximately rectangular hysteresis loop, while

the region of the wire which is under tension has an oblique loop with hardly any knee visible in the respective branches. The resultant loop for the entire wire would be obtained by superposition of the two loops.

The compressed half of the material of the wire maintains an almost constant intensity of magnetization as the field is decreased from a saturation value to zero; during this same field change the stretched part of the wire decreases its magnetization from saturation to a relatively

<sup>1</sup> R. Forrer, *J. de physique* **7**, 109 (1926); **10**, 247 (1929).

<sup>2</sup> M. Kersten, *Zeits. f. Physik* **71**, 553 (1931).